GLAZER, A. M. (1972*a*). *J. Appl. Cryst.* **5**, 420–423.
GLAZER, A. M. (1972*b*). *Acta Cryst.* B**28**, 3384–3392.
GLAZER, A. M. & MEGAW, H. D. (1972). *Phil. Mag.* **25**, 1119–1135.
ISMAILZADE, I. G. (1963). *Kristallografiya*, **8**, 363–367.
LEFKOWITZ, I., ŁUKASZEWICZ, K. & MEGAW, H. D. (1966). *Acta Cryst.* **20**, 670–683.
MILLEDGE, H. J. (1966). *Acta Cryst.* **21**, A220.
SAKOWSKI-COWLEY, A. C. (1967). Ph. D. Thesis, Univ. of Cambridge.
SAKOWSKI-COWLEY, A. C., ŁUKASZEWICZ, K. & MEGAW, H. D. (1969). *Acta Cryst.* B**25**, 851–865.
SOLOV'EV, S. P., VENEVTSEV, YU. N. & ZHDANOV, G. S. (1961). *Kristallografiya*, **6**, 218–224.
TENNERY, V. J. (1965). *J. Amer. Ceram. Soc.* **48**, 537–539.
WOOD, E. A. (1951). *Acta Cryst.* **4**, 353–362.

*Acta Cryst.* (1973). A**29**, 495

# Directions of Dislocation Lines in Crystals of Ammonium Hydrogen Oxalate Hemihydrate Grown from Solution

BY H. KLAPPER* AND H. KÜPPERS

*Institut für Kristallographie der Universität Köln, 5 Köln 41, Germany (BRD)*

(*Received* 24 *October* 1972; *accepted* 19 *March* 1973)

The defect structures in elastically highly anisotropic crystals of ammonium hydrogen oxalate hemihydrate, $NH_4HC_2O_4.\frac{1}{2}H_2O$, space group *Pnma*, have been studied by X-ray topography. Most of the dislocation lines visible on the topographs are straight and show clearly defined directions which depend on Burgers vector and on growth direction. Burgers vectors parallel to [100], [010], [001], ⟨101⟩ and ⟨011⟩ have been observed. For these Burgers vectors, the variation of energy factor $K$ with direction and the preferential directions of the corresponding dislocation lines in various growth sectors have been calculated. In most cases, observed and calculated directions agree well. The directions of a few dislocations tend to align parallel to low-indexed (symmetry) directions. The influence of the elastic anisotropy on the directions of the dislocation lines as well as the possibility of determining the Burgers vectors from observed preferential directions is discussed.

## Introduction

In crystals grown from solution, straight dislocation lines with typical, in general non-crystallographic, directions have been observed (Lang, 1967; Miuskov, Konstantinova & Gusev, 1969; Authier, 1972; Izrael, Petroff, Authier & Malek, 1972; Klapper, 1971, 1972*a*). These preferential directions depend on Burgers vector and on the growth direction of the growth sector concerned. The dependence on growth direction is easily observable when a dislocation penetrates a boundary between different growth sectors: the dislocation line is deflected into a direction which is characteristic of the new growth sector. As previously shown (Klapper, 1971, 1972*a*), those preferential directions may be explained by the following assumption. A dislocation, ending at a growing surface, will proceed into the newly grown layer in such a direction that the elastic energy of the region disturbed by the dislocation within this layer, or, which is the same, the energy per unit growth length, is minimum. Taking into account the elastic anisotropy of the crystals, calculations have been made for dislocations in benzil (Klapper, 1972*b*) and thiourea (Klapper, 1972*b*). Calculated and observed directions agree well.

In this work an investigation of the preferential directions of dislocation lines in crystals of orthorhombic ammonium hydrogen oxalate hemihydrate (AHO), $NH_4HC_2O_4.\frac{1}{2}H_2O$, which exhibit a high elastic anisotropy, is presented. The elastic constants (unit: $10^{11}$ dyne cm$^{-2}$) and lattice parameters are (Küppers, 1972*b*, 1973):

| | | |
|---|---|---|
| $c_{11}=$ 6·71 | $c_{12}=$ 1·485 | $c_{44}=0{\cdot}383$ |
| $c_{22}=$ 4·14 | $c_{13}=$ 0·749 | $c_{55}=0{\cdot}592$ |
| $c_{33}=$ 1·48 | $c_{23}=$ 1·30 | $c_{66}=0{\cdot}973$ |
| $a=11{\cdot}33$ | $b=12{\cdot}23$ | $c=6{\cdot}90$ Å. |

Evidently, the ratio of maximum to minimum longitudinal elastic stiffness is $c_{11}/c_{33}=4{\cdot}5$.

It is the purpose of this study to compare calculated and observed directions and to find out to what extent the observations of preferential directions can be used to determine the Burgers vector. The morphology of the crystals is shown in Fig. 1.

## Theory and calculations

The elastic energy $W$ per unit growth length is written (Klapper, 1972*b*):

$$W(\mathbf{e},\mathbf{l},\mathbf{n},c_{ij})=E(\mathbf{e},\mathbf{l},c_{ij})\cos\alpha$$

* Present address: Institut für Kristallographie der Technischen Hochschule Aachen, 51 Aachen, Germany (BRD).

($E$=elastic energy per unit length of the dislocation line, **e**=direction* of Burgers vector **b**, **l**=direction of the dislocation line, **n**=growth direction, $c_{ij}$=elastic constants, $\alpha$=angle between **l** and **n**). The direction $\mathbf{l}_0$, which is characterized by minimum $W$, depends on direction **e** of the Burgers vector, on growth direction **n**, and on the elastic constants $c_{ij}$:

$$\mathbf{l}_0=\mathbf{l}_0(\mathbf{e},\mathbf{n},c_{ij}).$$

The elastic energy $E$ per unit length of the dislocation line is given by Foreman (1955) and Hirth & Lothe (1968):

$$E(\mathbf{e},\mathbf{l},c_{ij})=\frac{K(\mathbf{e},\mathbf{l},c_{ij})}{4\pi}\,.\,|\mathbf{b}|^2.\ln\,(R/r)$$

($K$='energy factor', $r$=inner, $R$=outer cut-off radius). In the following, it is assumed that, for a dislocation with constant Burgers vector **b**, the dependence of the energy $E$ on the direction **l** is determined solely by the energy factor. A possible variation of the factor ln $(R/r)$ with **l** is neglected. Thus, we consider only the energy factor $K$ and the 'energy factor per unit growth length' $K_w=K\cos\alpha$.

In the numerical calculations of the energy factor $K$ we follow the outlines of Eshelby, Read & Shockley (1953), using a computer program. The variations of $K$ and $K_w$ with direction **l** were calculated in angular steps of 5°. The preferential directions were then determined within a smaller interval by varying **l** in steps of 1°.

In Fig. 2, the angular variation of the energy factor $K$ of dislocations with Burgers vectors [100], [010], [001] and [011] in the planes (100), (010) and (001) is plotted in polar coordinates. The numerical values of $K$ for directions parallel to the twofold axes of the crystal are given in Table 1. Fig. 3 shows some examples of the variation of $K_w=K\cos\alpha$ for dislocations with Burgers vectors [010], [001], and [011] in various growth sectors. In Fig. 4 and Table 2 calculated and observed directions are compared.

* The directions are represented by unit vectors.

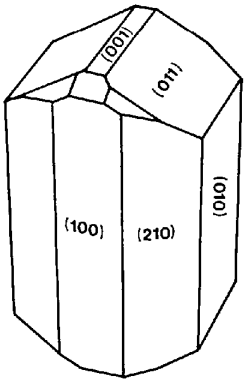


Fig. 1. Morphology of ammonium hydrogen oxalate hemihydrate.

Table 1. *Energy factor* $K$ ($10^{11}$ dyne cm$^{-2}$) *of dislocations with various Burgers vectors* **b** *for directions parallel to the twofold axes of the crystal*

| **l** | **b** | [100] | [010] | [001] |
|---|---|---|---|---|
| [100] | | 0·759 | 0·977 | 0·584 |
| [010] | | 1·696 | 0·610 | 0·796 |
| [001] | | 2·160 | 1·697 | 0·476 |

## Experimental results

Large single crystals were prepared by evaporation from aqueous solution (Küppers, 1972*a*). 14 plates parallel to (100), (010) and (001) were cut from two crystals and studied by X-ray topography using the Lang (1959) technique. The thickness of the plates ranged between 1 and 1·6 mm. All exposures were made with Mo $K\alpha_1$ radiation ($\lambda$=0·709 Å). The linear absorption coefficient for this wavelength is $\mu_0$=1·73 cm$^{-1}$. Reflexions 200, 040, 002, {303}, {220} and {022} were used.

In the following section some X-ray topographs, which present the characteristic features of the defect structures in AHO, are reproduced and described. Dislocations with the same Burgers vector are denoted by the same letters, those of different geometry are distinguished by different indices. The Burgers vectors and preferential directions are listed in Table 2. The observed and calculated directions are characterized by the angle $\varphi$ between these directions and the axes [100] or [001], which are vertical in Figs. 5–10. Most of the Burgers vectors have been determined with the aid of the visibility rules of dislocations images in X-ray topographs (**g** . **b** criterion, **g**=diffraction vector) (Lang, 1959; Newkirk, Bonse & Hart, 1967).

### (010) *plates* (*Fig.* 5)

Fig. 5 shows two plates parallel to (010), which contain regions grown on the faces (001), (101) and (100). Inclusions, mechanical defects on the faces of the plates, a crack and dislocations are visible. The dislocation lines labelled $C$ have a Burgers vector **b** ∥ [001]. They change direction when penetrating the boundary between the (001)- and the (101)-growth sectors. In both sectors the observed directions, which are sharply defined, agree within the accuracy of measurement with the theoretical directions [Fig. 4(*a*), Table 2].

The dislocations $A_1$, $B_1$ show in reflexion 200 [Fig. 5(*b*)] a broad and sometimes double contrast. We suppose them to be pure edge with **b** ∥ [100] or [010]. The observed direction coincides with the calculated one.

The dislocation lines $B_3$ and $C_3$ are pure edge, and Burgers vectors **b** ∥ [010], [001] and ⟨011⟩ are possible. Whichever of these vectors is correct, the theoretical and observed directions coincide (Table 2). Because of the strong contrast in reflexions 002 and {022}, **b** should be parallel to [001]. This is assumed to be the case for the lines $C_3$, which show a double image in Fig. 5(*a*). Both lines of the pair $B_3$ have a single contrast and are supposed to have the same **b**. The lower

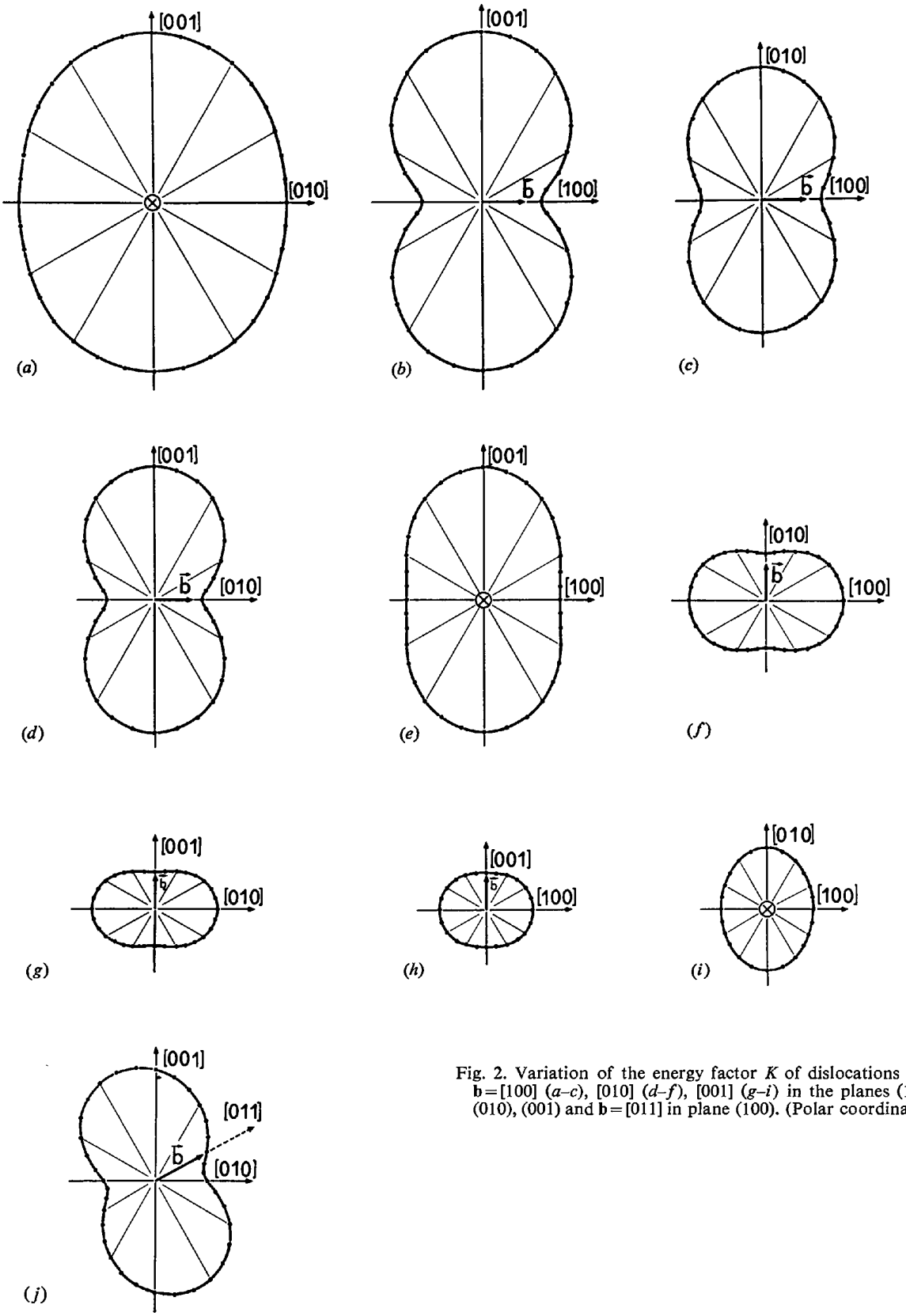


Fig. 2. Variation of the energy factor $K$ of dislocations with $\mathbf{b}=[100]$ (*a–c*), [010] (*d–f*), [001] (*g–i*) in the planes (100), (010), (001) and $\mathbf{b}=[011]$ in plane (100). (Polar coordinates).

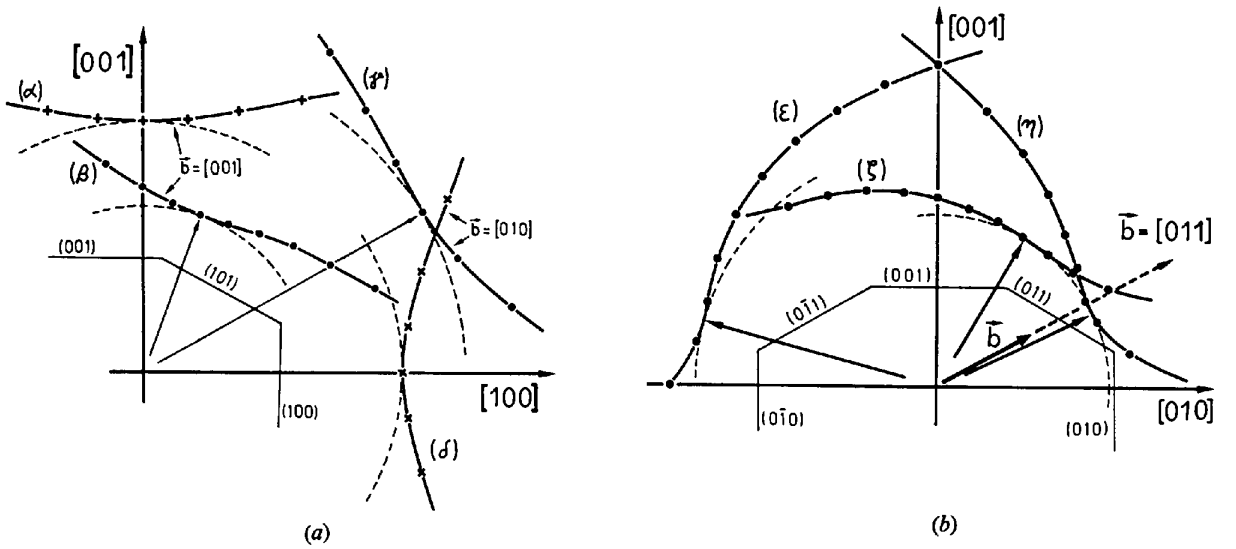


Fig. 3. Variation of the energy factor per unit growth length $K_w = K \cos \alpha$ (polar coordinates, arbitrary units). (*a*) plane (010): **b**=[001], sectors (001) ($\alpha$) and (101) ($\beta$); **b**=[010], sectors (101) ($\gamma$) and (100) ($\delta$). (*b*) plane (100): **b**=[011], sectors (0$\bar{1}$1) ($\varepsilon$), (001) ($\zeta$) and (011) ($\eta$). The directions of minimum $K_w$ are denoted by arrows.

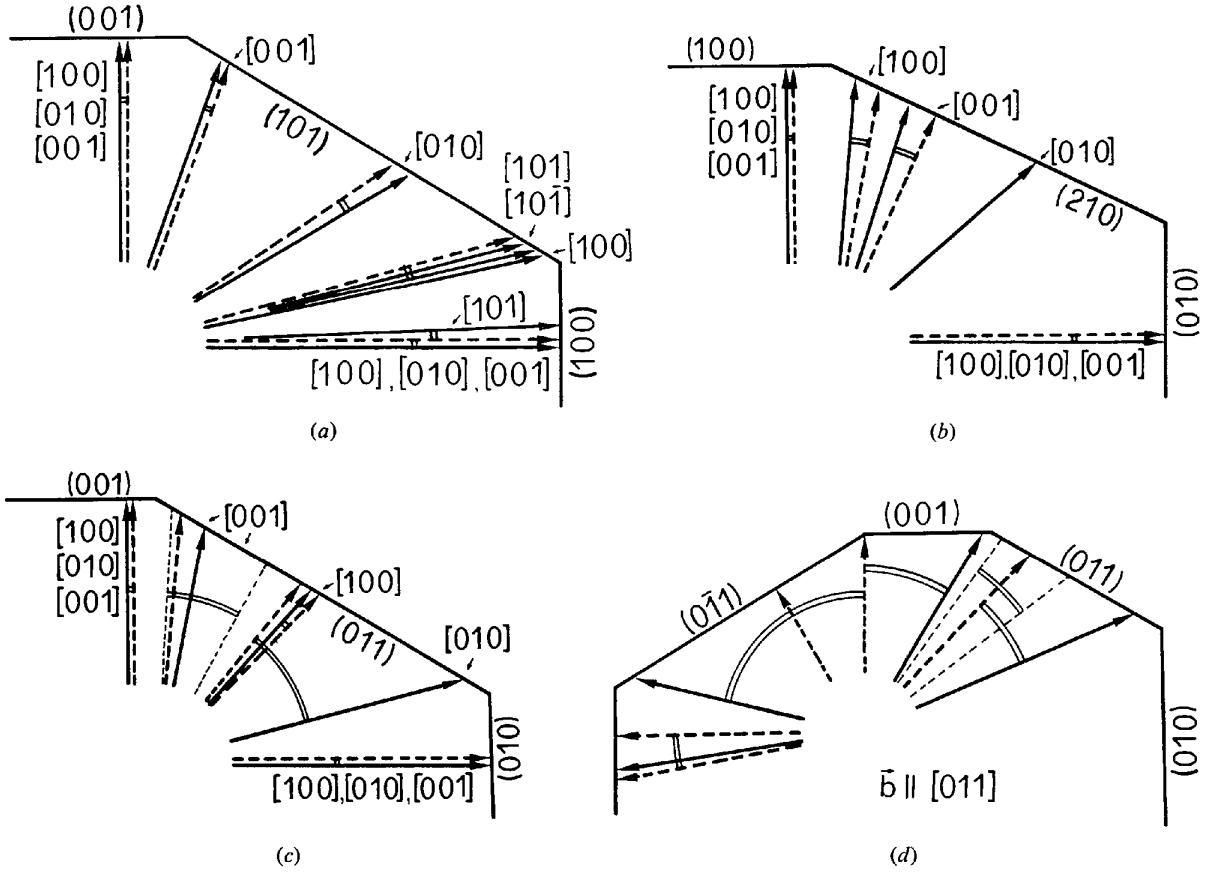


Fig. 4. Calculated (→) and observed (→) directions of dislocation lines with **b**∥[100], [010], [001] and [011] in various growth sectors. The directions belong to those sectors at the face of which the representing arrows end. Corresponding calculated and observed directions are connected with double arcs.

line of this pair has a short line element $B_4$ lying in sector (101), with direction $\varphi = 56°$, which vanishes in reflexion 303. Therefore it should have a Burgers vector $\mathbf{b} \parallel [010]$. This is supported by the close coincidence of the line element $B_4$ with the calculated direction. For dislocations of this type, however, the lines $B_3$ show in Fig. 5(*a*) a stronger contrast than is to be expected. A similar observation is made for dislocations $A_4$, $A_6$ in Fig. 8. The lines $A_4$ vanish in reflexion 040, whereas those labelled $A_6$ approximately do so in the 022 reflexion. From this, $\mathbf{b} \parallel [100]$ can be concluded, and this is confirmed by the agreement of observed and calculated directions.

For the dislocation lines $E_1$, $E_2$ a significant contrast minimum is not recognizable in reflexions 040, 002, {303} and {022}. Their directions in sectors (100) and (101) agree well with those calculated for $\mathbf{b} = [100]$, [101] and [10$\bar{1}$] [Fig. 4(*a*), Table 2]. The observed contrast fits better with the two latter Burgers vectors, which are most probably correct. In the case of $\mathbf{b} \parallel [101]$ the preferred direction in sector (101) does not lie between the growth normal and the Burgers vector, as is the rule (see Discussion). This is owing to the large approximately 30° angle between the Burgers vector [101] and the direction of minimum $K$, which lies close to [100] ($\varphi = 88°$).

The lines $B_2$ exhibit a similar appearance to $B_4$, but do not completely vanish in reflexion 303. Their Burgers vector is probably parallel to [010].

(001) *plates* (*Fig.* 6)

The plates of Fig. 6(*a*,*b*) are cut through the seed crystal Se. Both specimens contain mainly regions grown on the faces {100}, {010} and {210}. Growth sector boundaries (Gr) and growth bands in {210} sectors are faintly visible.

Bundles of closely packed dislocations originate from inclusions at the surface of the seed. In the sectors {100} and {010} both pure-edge and pure-screw dislocations could be identified. Bundle $A_4$, $C_5$ was found to consist of pure-edge dislocations with $\mathbf{b} \parallel$ [100], [001] or ⟨101⟩. The dislocations $A_7$ are also pure edge with $\mathbf{b} \parallel [100]$.

The pure-edge dislocations $C_4$ ($\mathbf{b} \parallel [001]$) in sectors {210} are faintly visible in reflexions of zone [001] and show minimum contrast in Fig. 6(*b*). Their direction ($\varphi = 24°$) lies close to the growth normal ($\varphi = 24{,}5°$). The theoretical direction is $\varphi = 18°$.

The dislocation lines $B_5$ originate in the seed crystal and change direction when passing from a {111} sector into a {210} sector. Here they are parallel to the axis [100]. They maintain this direction when passing into a {100} sector. The determination of their Burgers vector is not certain. As they show a wide and

Table 2. *Calculated and observed directions* $\mathbf{l}_0$ *in different growth sectors*

$\varphi$ is the angle between $\mathbf{l}_0$ and the direction [*uvw*] in the plane (*hkl*). Mean values of $\varphi$ in brackets. The labels of the corresponding dislocations in Figs. 5–9 are given in the last column. The directions marked with * are influenced by the lattice structure (see discussion).

| Sector | b | [*uvw*] | (*hkl*) | $\varphi_{calc}$(°) | $\varphi_{obs}$(°) | Fig. | Label |
|---|---|---|---|---|---|---|---|
| {100} | [100] | Calc. and obs. $\mathbf{l}_0 \parallel [100]$ | | | | 6 | $A_2$ |
| | [010] | | | | | 5,6 | $B_3, B_5$ |
| | [001] | | | | | 5 | $C_3$ |
| | ⟨011⟩ | Calc. $\mathbf{l}_0 \parallel [100]$ | | | | – | – |
| | ⟨101⟩ | [001] | (010) | 88 | 90 | 5 | $E_1$ |
| {010} | [100] | Calc. and obs. $\mathbf{l}_0 \parallel [010]$ | | | | 6,8 | $A_7, A_4$ |
| | [010] | | | | | 8 | $B_7$ |
| | [001] | | | | | 6,8 | $C_5$ |
| | ⟨101⟩ | Calc. $\mathbf{l}_0 \parallel [010]$ | | | | – | – |
| | ⟨011⟩ | [001] | (100) | 98 | 100,90* | 8 | $D_5$ |
| {001} | [100] | Calc. and obs. $\mathbf{l}_0 \parallel [001]$ | | | | 5 | $A_1$ |
| | [010] | | | | | 5 | $B_1$ |
| | [001] | | | | | 5,7 | $C_1$ |
| | ⟨011⟩ | [001] | (100) | 33 | 0* | 8,9 | $D_2$ |
| {101} | [100] | [001] | (010) | 79 | | – | – |
| | [010] | | | 59 | 56 | 5 | $B_2, B_4$ |
| | [001] | | | 20 | 20 | 5 | $C_2$ |
| | [101] | | | 76 | | | |
| | [10$\bar{1}$] | | | 77 | 75 | 5 | $E_2$ |
| {210} | [100] | [100] | (001) | 5 | 10 | 6 | $A_5$ |
| | [010] | | | 49 | 0* | 6 | $B_5$ |
| | [001] | | | 18 | 24 | 6 | $C_4$ |
| {011} | [100] | [001] | (100) | 43 | 45 | 8 | $A_6$ |
| | [010] | | | 76 | 38 | 7 | $B_6$ |
| | [001] | | | 13 | 6,4–35 | 7,8 | $C_6, C_7$ |
| (0$\bar{1}$1) | [011] | [001] | (100) | 75 | 0–75 (32)* | 8,9 | $D_1, D_4$ |
| (011) | | | | 64 | 36–55 (43)* | 8,9 | $D_3$ |

intense double contrast in reflexion 040, a lower, but equal contrast in both reflexions {220} and minimum visibility in 200 [Fig. 6(*b*)], **b** ∥ [010] is probable. However, the images of such dislocations should completely vanish in reflexion 200. On the other hand, in other plates dislocation lines with just this geometry ($B_5$) and strictly the contrast characteristic of **b** ∥ [010] occur. In sector {210} their theoretical direction is $\varphi = 49°$, Here a great discrepancy between observed and calculated directions is found. This may be caused by the lattice structure of the crystal (see Discussion).

Both plates of Fig. 6(*a*,*b*) contain a small region grown on a face {011} (label *W*). Here dislocation lines penetrating the plate are observed.

(100) *plates* (*Figs.* 7–10)

The topograph in Fig. 7(*a*) shows many dislocations $C_6$ originating from crowds of small inclusions, containing mother liquor, arranged in planes parallel to the growth face $(0\bar{1}1)$. They have pure or nearly pure-screw character with **b** ∥ [001]. A slight change in direction occurs when the lines pass from the $(0\bar{1}1)$ section ($\varphi = 6°$) into the (001) sector ($\varphi = 0°$). Some of them are slightly curved and assume, close to the $(0\bar{1}1)$ surface, a direction $\varphi \simeq 10°$. The calculated angle is $\varphi = 13°$.

In Fig. 7(*b*), which shows a section of a (100) plate cut from another crystal, dislocation lines $C_7$ of the same type as just described (**b** ∥ [001]) are visible. Here some of them have a zigzag-like course, with the directions of the line elements varying in the interval $\varphi =$ 4–35°. The theoretical direction is close to the centre of this interval, which in Fig. 4(*c*) is marked by the dashed lines. Most of the line elements have direction $\varphi \simeq 4°$. The reasons for this geometry of these dislocation lines were not discovered. It is noteworthy that it is observed in only one of the two crystals we have studied.

Moreover, in Fig. 7(*b*) two dislocation lines $B_6$ (**b** ∥ [010], lying in the sector (011), are faintly visible. They are not strictly rectilinear. Their mean direction is $\varphi \simeq 38°$. Here the deviation from the theoretical direction ($\varphi = 76°$) is rather high. Nevertheless, the observed direction lies between Burgers vector and growth direction (see rule 3 in the Discussion). The contrast of the images of these dislocations is not homogeneous along the lines, which, in reflexion 002, are partly invisible. This indicates a variable decoration which might have occurred during crystal growth and influenced the directions of the lines.

Very interesting features are revealed by the dislocations labelled *D* (Figs. 8, 9). In Fig. 9 they originate in the interior of the seed crystal Se and proceed into the grown crystal. Their Burgers vector is parallel to [011]. This is, next to [100], the direction of the shortest lattice translation in $(0\bar{1}1)$, which is a plane of perfect cleavage. Most dislocations in the bundle *T* are of this type. In sector $(0\bar{1}1)$ they frequently have a zigzag-like appearance (labels $D_1$, $D_4$ in Figs. 8, 9), one line element being exactly parallel to [001] and the other having directions between $\varphi = 0$ and 75°. The mean direction is approximately parallel to the growth direction [Fig. 4(*d*)]. Here they have pure or predominant edge character. Long line elements of these dislocations parallel to [001] also frequently occur, as can be seen from group $D_2$ [Fig. 8(*b*)], which lies half in sector $(0\bar{1}1)$ and half in sector (001). A change in directions of these lines when passing the boundary between these sectors is not observed. Close to the $(0\bar{1}1)$ surface a deflection towards the growth direction occurs.

In sector (001), the dislocation lines with **b** ∥ [011] are exactly parallel to [001] ($\varphi = 0°$, label $D_2$). The theoretical direction is $\varphi = 33°$ (see Discussion).

The dislocation lines $D_3$ in sector (011) have predominant screw character. They are not strictly rectilinear, and have directions ranging in the interval $\varphi \simeq$ 36–55° [dashed lines in Fig. 4(*d*)], with a mean angle $\varphi \simeq 43°$. This deviates strongly from the calculated direction ($\varphi = 65°$), but lies between Burgers vector and growth direction.

Some of the lines labelled *D* (**b** ∥ [011]) enter the growth sectors {010} and are deflected in the direction [010]. Here they reveal a strong contrast in both reflexions 002 and 040 [Fig. 8(*a*,*b*)]. The lines $D_5$, which vanish completely in one of the reflexions {022}, have also **b** ∥ [011]. Their direction coincides closely with the calculated one (Table 2).

Fig. 10 shows some pure-screw dislocations (**b** ∥ [010]) parallel to the growth direction of sector (010). They reveal some half-circular loops, which have been produced by a partial movement of the dislocation lines after crystal growth was complete.

## Discussion

*Influence of elastic anisotropy*

The effect of elastic constants on the preferential directions $\mathbf{l}_0$ will be demonstrated in two extreme cases: elastic isotropy and high elastic anisotropy.

In an elastic isotropic medium, the energy factor is $K_s = \mu$ for pure screw, and $K_e = \mu/1 - \nu$ for pure-edge dislocations of any orientation of the dislocation line perpendicular to Burgers vector ($\mu$ = shear modulus, $\nu$ = Poisson's ratio). Because of $0 < \nu < \frac{1}{2}$, the relation $1 < K_e/K_s < 2$ holds. For this reason the variation of $K$ with direction **l** is rather small, and the variation of $K_w = K \cos \alpha$ is mainly determined by the factor $1/\cos \alpha$, which is a minimum for the direction parallel to the growth normal **n**. As a consequence, the preferred directions $\mathbf{l}_0$ will lie rather close to the growth direction **n**. In particular, since $K = K_e$ is constant in the plane perpendicular to the Burgers vector **b**, in growth sectors with **n** normal to **b**, $\mathbf{l}_0$ should exactly coincide with **n** (pure-edge dislocation). An example of a rather small variation in $K$, similar to the case of elastic isotropy, is represented in AHO by dislocations with **b** = [001] [Fig. 2(*h*,*i*)]. These dislocations have in sectors {101} [Fig. 5(*a*,*c*): label $C_2$] and {210} [Fig.

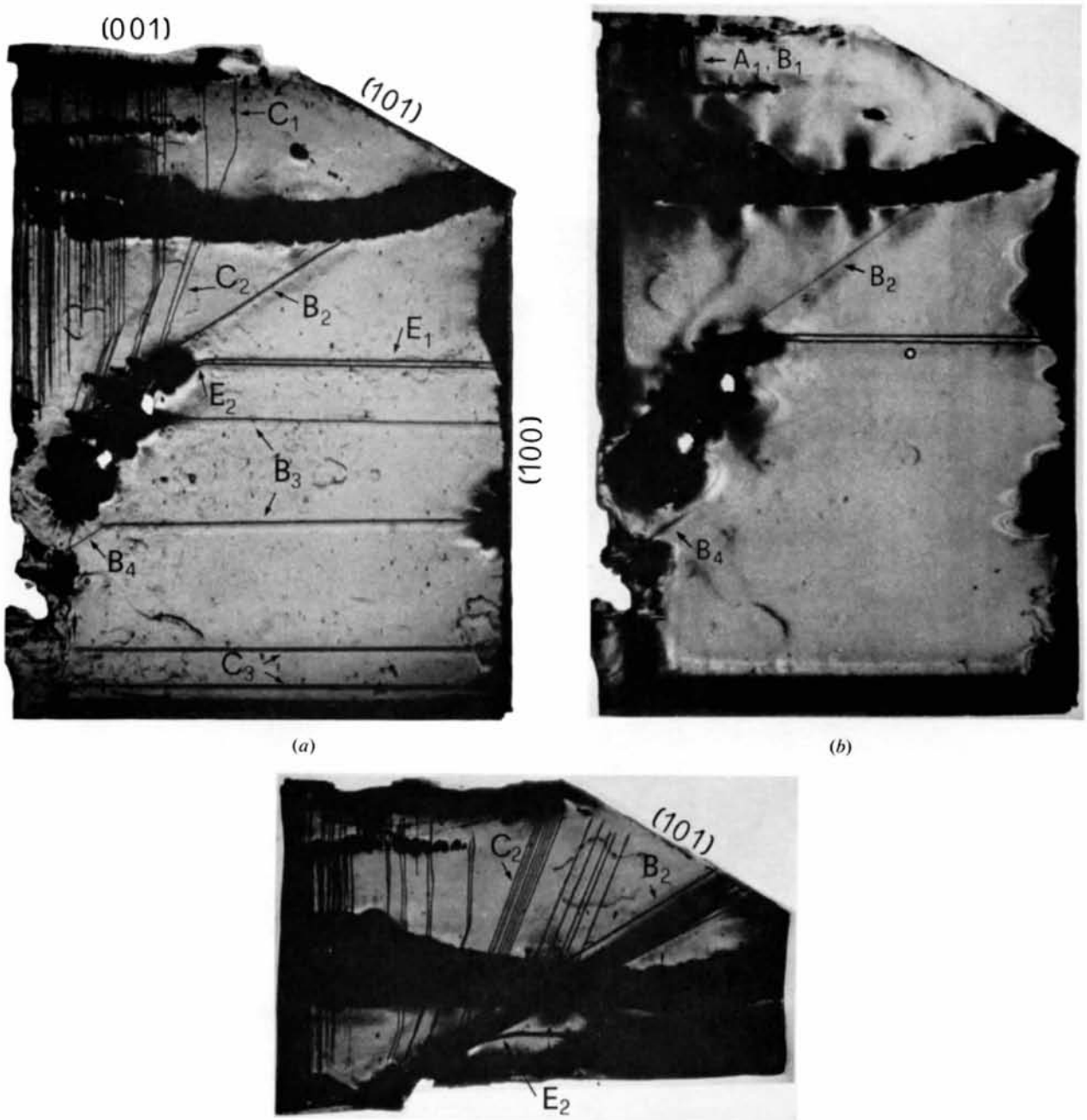


(a) (b)

(c)

Fig. 5. (010)-plate, 1·4 mm thick, horizontal dimension 11 mm. (*a*) and (*c*) reflexion 002; (*b*) same plate as in (*a*), but reflexion 200.

[*To face p.* 500

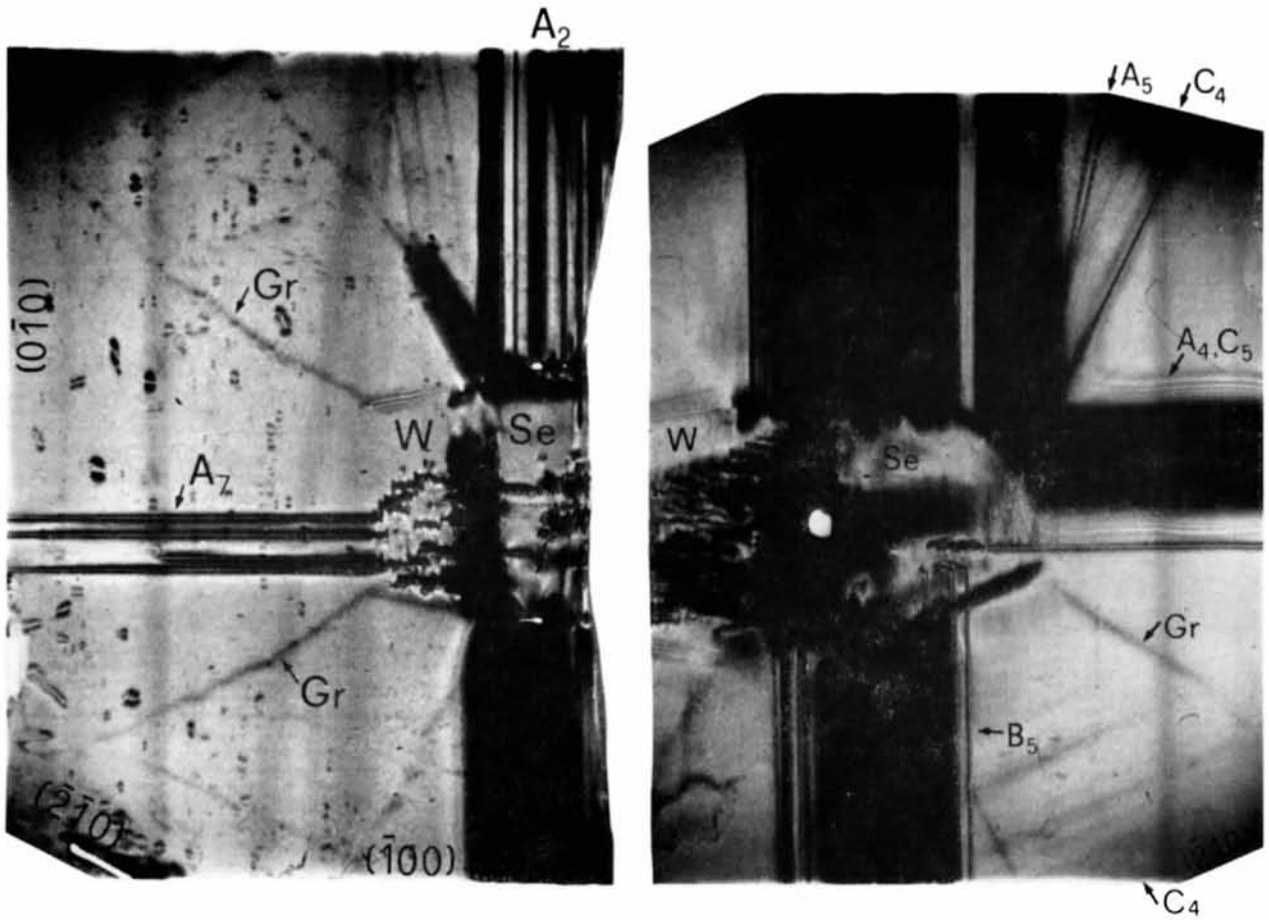


(*a*) (*b*)

Fig. 6. (001) plates, about 1·2 mm thick, horizontal dimension 18 mm. Both reflexions 200.

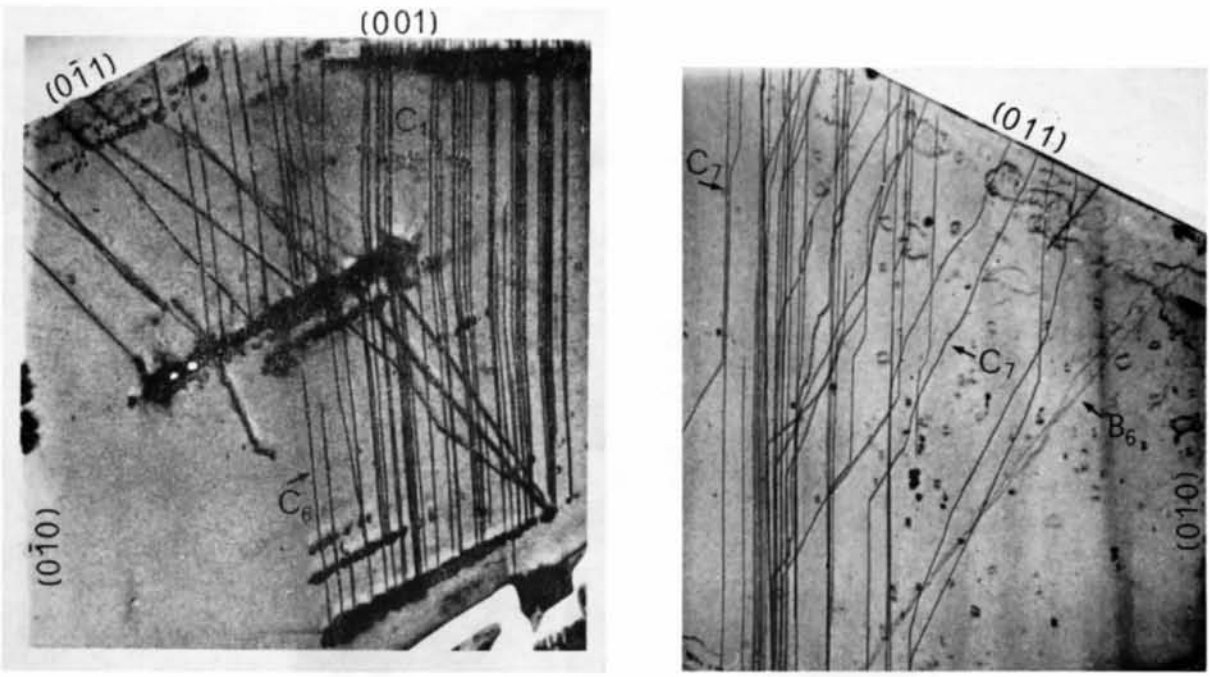


(*a*) (*b*)

Fig. 7. Sections from (100) plates. (*a*) 1·2 mm thick, horizontal dimension of section: 8·5 mm. (*b*) 1 mm thick, horizontal dimension 11 mm. In both (*a*) and (*b*) reflexion 002.

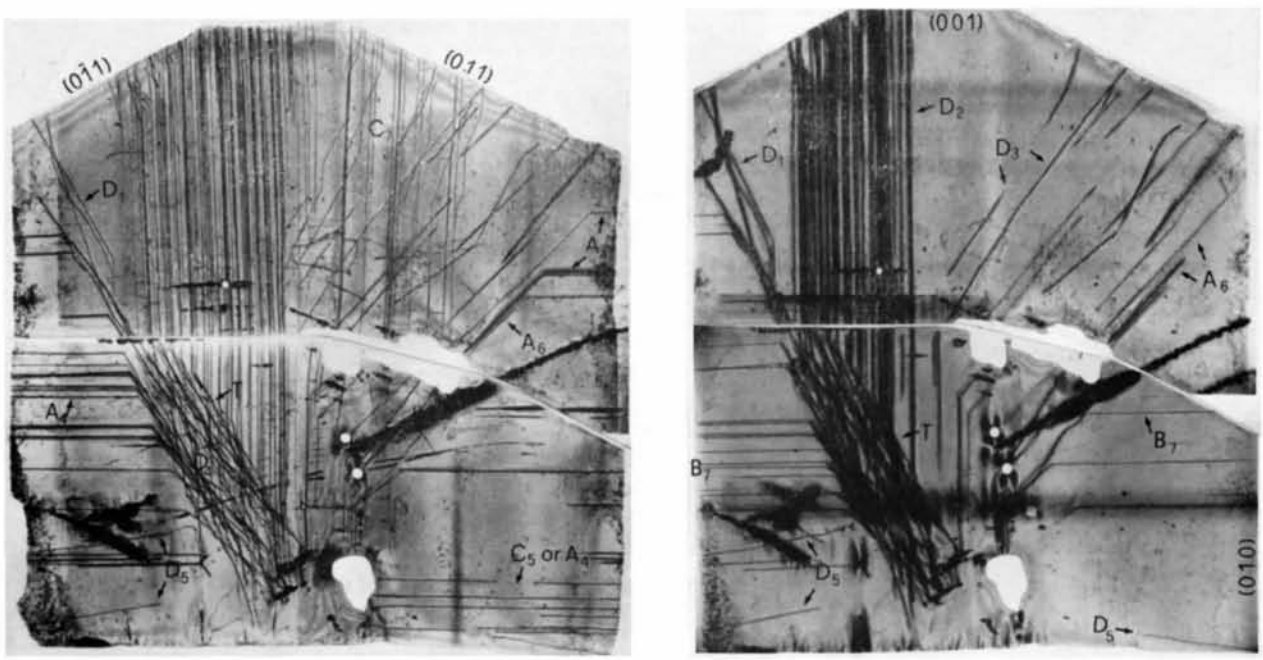


(*a*) (*b*)

Fig. 8. (100) plate, 1·5 mm thick, horizontal dimension 22 mm. (*a*) reflexion 002, (*b*) 040.

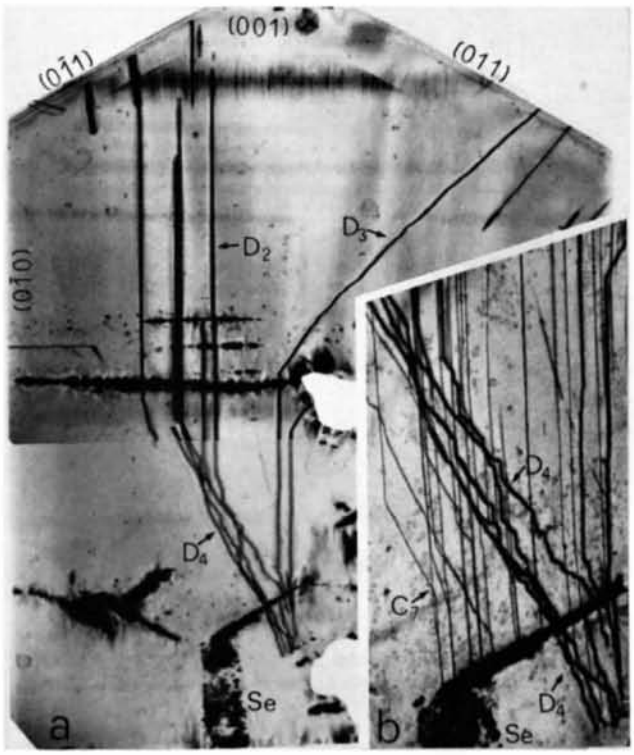


Fig. 9. (100) plate, 1·3 mm thick; (*a*) horizontal dimension 20 mm, reflexion 040. (*b*) enlarged section of the same plate with dislocation group $D_4$, however in reflexion 022. Dislocations $C_7$ are of the same type as in Fig. 7(*b*).

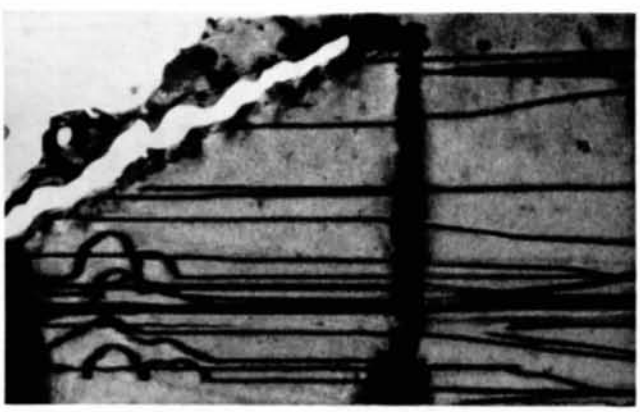

Fig. 10. (100) plate, 1·5 mm thick, horizontal dimension of reproduced field 7 mm, [001] vertical, reflexion 040.

6(*b*): label $C_4$] observed directions rather close to **n** ($\Delta\varphi \simeq 11°$ and $\Delta\varphi \simeq 0°$ respectively; $\Delta\varphi$ is the angle between **n** and $\mathbf{l}_0$).

In crystals of high elastic anisotropy, values of $K_e/K_s > 2$ and, accordingly, greater variations in $K$, may occur (examples: $K_e/K_s = 2{\cdot}85$ for dislocations with $\mathbf{b} = [100]$ in AHO [Fig. 2(*b*)]; $K_e/K_s \simeq 6$ for $\mathbf{b} = [010]$ in thiourea). $K_e$ is no longer constant in the plane perpendicular to **b** [Fig. 2(*a,e,i*)] and may vary considerably with direction [Fig. 2(*e*)]. As a consequence, larger angles between preferential direction $\mathbf{l}_0$ and growth normal **n** are observed [example: Fig. 5(*a,b,c*): dislocations labelled $E_2$ in sector (101), $\Delta\varphi \simeq 44°$]. Furthermore, pure-edge dislocation lines not parallel to **n** may appear [example: Fig. 8(*a,b*): label $A_6$ in sector (011), $\Delta\varphi \simeq 15°$].

*Influence of lattice structure*

In the formulae used in the preceding calculations of elastic energy a continuous medium was assumed. As has been pointed out in a previous paper (Klapper, 1972*b*), the lattice structure may also influence the directions of the dislocation lines. In AHO we have observed this influence for dislocations with $\mathbf{b} = \langle 011 \rangle$ and [010] where the lines (or the line elements) do not follow the calculated but other, low-indexed directions ([001] and [100] respectively) [label $D_2$, $D_4$ in Figs. 8, 9 and $B_5$ in Fig. 6(*b*)]. Similar observations have been made in crystals with the diamond structure, such as silicon or germanium (Dash, 1957; Meyer, 1962; Authier & Lang, 1964). In these materials the dislocation lines tend to align themselves parallel to $\langle 110 \rangle$ directions, which are characterized by a low Peierls energy (Holt & Dangor, 1963). It seems that during crystal growth the influence of these 'Peierls troughs' may in some cases dominate over the effects outlined in the preceding sections and may affect the directions of the dislocation lines.

From topographic evidence, [001] is supposed to be a favoured lattice direction of this kind for dislocations with $\mathbf{b} \parallel \langle 011 \rangle$. For a tentative estimation of the competing influences of this direction and that for minimum $K_w$, the difference $\Delta K_w = K_w(\mathbf{l}_f) - K_w(\mathbf{l}_0)$ ($\mathbf{l}_f$, favoured lattice direction, $\mathbf{l}_0$, calculated preferential direction) will be considered. Some value of $\Delta K_w$ are presented in Table 3.

Table 3. *Some values of the energy factor per unit growth length, $K_w$, for calculated preferential directions $\mathbf{l}_0$ [$K_w(\mathbf{l}_0) = minimum$] and for favoured lattice directions $\mathbf{l}_f$ in different growth sectors* ($10^{11}$ dyne cm$^{-2}$)

| **b** | $\mathbf{l}_f$ | Sector | $K_w(\mathbf{l}_f)$ | $K_w(\mathbf{l}_0)$ | $\Delta K_w$ |
|---|---|---|---|---|---|
| [011] | [001] | (0$\bar{1}$1) | 1·623 | 1·220 | 0·403 |
| | | (001) | 1·426 | 1·293 | 0·123 |
| | | (011) | 1·623 | 0·863 | 0·760 |
| [011] | [010] | (010) | 0·659 | 0·627 | 0·032 |
| [010] | [100] | (210) | 1·073 | 0·893 | 0·180 |
| | | (100) | 0·977 | 0·977 | 0·0 |
| | | (101) | 1·872 | 1·304 | 0·568 |

In sector (0$\bar{1}$1) [Fig. 4(*d*)], $K_w$ increases rather slowly when the dislocation-line direction moves from $\mathbf{l}_0$ ($\varphi = 75°$) towards [001] ($\varphi = 0°$). Thus we should expect a certain spread of directions within this interval. This is actually observed in those line elements of the zigzag-like dislocation lines with mean direction close to **n** (Figs. 8, 9: labels $D_1$, $D_4$). The difference $\Delta K_w$ is 0·403* in this sector. Here the influences of lattice structure and minimum $K_w$ seem to be of the same order and affect the directions to an equal extent. In this way the zigzag-like appearance of the dislocations with line elements either close to **n** or parallel to $\mathbf{l}_f \parallel$ [001] may be explained.

In sector (001) although a preferential direction $\mathbf{l}_0$ with $\varphi = 33°$ was calculated, all dislocations are observed to run exactly parallel to [001]. Here $\Delta K_w = 0{\cdot}123$ has a smaller value than in sector (0$\bar{1}$1), and the influence of the lattice structure on the dislocation-line direction is predominant.

In sector (011), however, $\Delta K_w = 0{\cdot}76$. Here a dislocation direction close to $\mathbf{l}_0$ is expected to be energetically more favourable than the direction [001]. This may be observed (Figs. 8, 9: label $D_3$): line elements parallel to [001] do not occur. Obviously, for dislocations with $\mathbf{b} \parallel [011]$, the difference $\Delta K_w \simeq 0{\cdot}4$ (due to the zigzag configuration) is a critical value which separates the ranges of predominance of the influences of the direction [001] and the minimum energy per unit growth length.

In sectors {010} the dislocation lines with $\mathbf{b} \parallel \langle 011 \rangle$ assume essentially two directions: $\varphi = 100$ or 90° [Fig. 4(*d*)]. Here the lattice direction [010] also seems to be favoured. Its influence on the dislocation-line directions, however, is apparently not as strong as that of direction [001] ($\Delta K_w = 0{\cdot}032$).

For dislocations with $\mathbf{b} \parallel [010]$ [Fig. 6(*b*): label $B_5$], [100] seems to be a favoured lattice direction. In sectors {111} the influence of minimum $K_w$ is stronger, whereas in {210} that of direction [100] is predominant. In the {210} sectors, $\Delta K_w$ (= 0·18) has a rather low value. Hence, the dislocations run parallel to [100]. In sectors {100}, both influences cooperate to align the dislocations parallel to [100]. Thus, a deflexion of these dislocation lines when passing the boundary between the {210} and the {100} sectors does not occur. Directions parallel to [100] have not been observed in sectors {101}. Here $\Delta K_w$ is equal to 0·568.

*Determination of Burgers vectors*

In X-ray topography, the Burgers vectors are usually determined with the aid of the **g** . **b** criterion. Sometimes, however, an unambiguous determination is not possible with this method. Since the preferential directions of dislocation lines in a certain growth sector are characteristic of the Burgers vector, the observation of such directions should yield some information on the direction of the Burgers vector. This should be

* Dimensions of $\Delta K_w$ are $10^{11}$ dyne cm$^{-2}$.

possible particularly in such cases where the dislocations penetrate a sector boundary, so that preferential directions in different growth sectors can be observed.

Relying on the knowledge of the elastic constants and on the availability of a computer program, we may consider 3 cases: I. If in a crystal Burgers vectors and corresponding preferential directions have once been determined with the aid of visibility rules, then in further X-ray topographic investigations Burgers vectors of these dislocations can be identified by their preferential directions $\mathbf{l}_0$, without necessarily taking additional exposures in different reflexions. In this study on AHO we have on occasion applied this method.

II. If elastic constants and growth directions of the crystal under investigation are known and if a computer program is available, the directions $\mathbf{l}_0$ may be calculated for various Burgers vectors and compared with observed ones. In this way, Burgers vectors of some dislocations in AHO which were not identified unambiguously by visibility rules could be confirmed by the close coincidence of observed and calculated directions [example: Fig. 8(*a*,*b*): label $A_6$ in sector (011)].

III. Even if the elastic constants are not known some general statements on preferential directions may be given. In a previous paper (Klapper, 1972*b*), three rules concerning these directions were derived under the assumption that the energy factor $K_s$ of a pure-screw dislocation is minimal and that of a pure-edge dislocation $K_e$ is maximal. These rules are:

1. If $\mathbf{b} \parallel \mathbf{n}$, then $\mathbf{l}_0 \parallel \mathbf{n}$ (pure-screw dislocation);
2. If $\mathbf{b} \perp \mathbf{n}$, then $\mathbf{l}_0 \parallel \mathbf{n}$ (pure-edge dislocation);
3. If $\mathbf{b} \not\parallel \mathbf{n}$, and $\mathbf{b}$ not $\perp \mathbf{n}$, then $\mathbf{l}_0$ lies between $\mathbf{n}$ and $\mathbf{b}$.

The results from the present work on a highly anisotropic crystal indicate some violations of rule 2 for dislocations with $\mathbf{b} \parallel [010]$ in sector {101} and $\mathbf{b} \parallel [100]$ in sector {011} (Figs. 5 and 8: labels $B_2$, $B_4$ and $A_6$) and also in thiourea for $\mathbf{b} \parallel [010]$ in sector {101} (Klapper, 1972*a*,*c*). Rule 2 holds, however, if a restriction is introduced as follows:

2. If $\mathbf{b} \perp \mathbf{n}$ and $\mathbf{n}$ is parallel to a (twofold) symmetry axis, then $\mathbf{l}_0 \parallel \mathbf{n}$.

If $\mathbf{b} \perp \mathbf{n}$ is parallel to, but $\mathbf{n}$ not parallel to, a symmetry axis, then $\mathbf{l}_0$ should lie between $\mathbf{n}$ and the direction of minimum $K_e$. This is true for the directions $\mathbf{l}_0$ of the edge dislocations just mentioned. In the case of low elastic anisotropy, $\mathbf{l}_0$ should lie close to $\mathbf{n}$.

These rules have proved to be obeyed for nearly all dislocations we have observed in AHO, even in such cases where great differences between calculated and observed directions appeared. The only exceptions are provided by those dislocations whose directions are predominantly influenced by the lattice structure, and possibly by the dislocation lines labelled $E_2$ (Fig. 5).

In order to discuss possible means of obtaining information on Burgers-vector directions in orthorhombic crystals with the aid of these rules, we shall consider some special cases:

When in sectors {100}, {010} and {001} preferred directions parallel to the growth normal $\mathbf{n}$ are observed, rules 1 and 2 should be applied. Accordingly, these dislocations are expected to be pure screw or pure edge with $\mathbf{b}$ parallel to one of the orthorhombic axes. This has been observed in AHO. A distinction between these possible Burgers vectors, however, cannot be made by the directions alone. Moreover, we have to account for the possibility that, as a consequence of the lattice structure, mixed dislocations parallel to $\mathbf{n}$ may occur (*i.e.* dislocations with $\mathbf{b} \parallel \langle 011 \rangle$ in sectors {001} of AHO). Hence, in this case, only little information can be gained from rules 1 and 2.

When in sectors {100}, {010} and {001} clearly defined preferential directions $\mathbf{l}_0$ non-parallel to $\mathbf{n}$ are observed, Burgers vectors $\mathbf{b} \parallel [100]$, [010] and [001] can, with high probability, be excluded. In such cases, rule 3 is applicable. $\mathbf{b}$ should be a low-indexed lattice vector between $\mathbf{l}_0$ and the normal to $\mathbf{n}$. Dependent on the observed $\mathbf{l}_0$ and on the growth sector concerned, Burgers vectors of type [011], [101] and [110] should be taken into consideration [*i.e.* dislocations with $\mathbf{b} \parallel \langle 011 \rangle$ in sector {010} of AHO (label $D_5$ in Fig. 8); $\mathbf{b} \parallel \langle 101 \rangle$ in sector {100} of thiourea (Klapper, 1972*a*, *c*)].

Similar considerations may be useful in determining the Burgers vectors of dislocations in the other growth sectors.

If elastic constants are available it may be favourable to calculate the numerical values of $K$ for special directions. This may be done in an elementary way without a computer. For directions parallel to the axis of orthorhombic crystals, the following equations can be used (for details, see Hirth & Lothe, 1968, p. 425):

$$K_e = (\bar{c}_{11} + c_{12}) \left[ \frac{c_{66}(\bar{c}_{11} - c_{12})}{c_{11}(\bar{c}_{11} + c_{12} + 2c_{66})} \right]^{1/2}; \quad \bar{c}_{11} = (c_{11} \cdot c_{22})^{1/2}$$

$$K_s = (c_{44} \cdot c_{55})^{1/2}.$$

For dislocations with $\mathbf{b}$ parallel to the orthorhombic axes, these values are extrema and give an idea how strongly the energy factor $K$ varies with direction. From this, we may get a rough qualitative estimation of the theoretically expected angle between $\mathbf{l}_0$ and the growth direction $\mathbf{n}$.

These considerations may be useful in getting information on Burgers-vector directions, as has been proved for dislocations in AHO, benzil (Klapper, 1972*b*), thiourea (Klapper, 1972*c*) and lithium formate hydrate (Klapper, 1973). On the other hand, the directions of dislocation lines may be strongly influenced by still other factors. Besides the effect of the lattice structure discussed above, the decoration of dislocation lines, long-range strain fields produced by other lattice defects occurring during crystal growth (growth bands, for example), and movement after crystal growth (Fig. 10) should be mentioned. As a conse-

quence of these additional effects there may be large differences between observed and theoretical directions, and curved dislocation lines may occur. In such cases the determination of Burgers vectors from the directions of dislocation lines is questionable or impossible.

### Conclusion

This study gives a further confirmation that the directions of grown-in straight dislocation lines are in many cases predominantly influenced by the tendency to minimize the elastic dislocation energy per unit growth length. Some consequences resulting from this theory and concerning the effect of elastic anisotropy and the determination of Burgers vectors, as well as the influence of the lattice structure are discussed. These subjects, however, require further investigations which this work may stimulate.

### References


AUTHIER, A. (1972). *J. Cryst. Growth*, **13/14**, 34–38.

AUTHIER, A. & LANG, A. R. (1964). *J. Appl. Phys.* **35**, 1956–1959.

DASH, W. C. (1957). *The Observation of Dislocations in Silicon* in *Dislocations and Mechanical Properties of Crystals*, p. 57–68. New York: Wiley.

ESHELBY, J. D., READ, W. T. & SHOCKLEY, W. (1953). *Acta Metall.* **1**, 251–259.

FOREMAN, A. J. E. (1955). *Acta Metall.* **3**, 322–330.

HIRTH, T. P. & LOTHE, J. (1968). *Theory of Dislocations*. New York: McGraw-Hill.

HOLT, D. B. & DANGOR, A. E. (1963). *Phil. Mag.* **8**, 1921–1936.

IZRAEL, A., PETROFF, J. F., AUTHIER, A. & MALEK, Z. (1972). *J. Cryst. Growth*, **16**, 131–141.

KLAPPER, H. (1971). *J. Cryst. Growth*, **10**, 13–25.

KLAPPER, H. (1972*a*). *J. Cryst. Growth*, **15**, 281–287.

KLAPPER, H. (1972*b*). *Phys. Stat. Sol.* (*a*), **14**, 99–106.

KLAPPER, H. (1972*c*). *Phys. Stat. Sol.* **14**, 443–451.

KLAPPER, H. (1973). *Z. Naturforsch*, **28a**, 614–623.

KÜPPERS, H. (1972*a*). *J. Cryst. Growth*, **15**, 89–92.

KÜPPERS, H. (1972*b*). *Acta Cryst.* A**28**, 522–527.

KÜPPERS, H. (1973). *Acta Cryst.* B**29**, 318–327.

LANG, A. R. (1959). *J. Appl. Phys.* **30**, 1748–1755.

LANG, A. R. (1967). *Advanc. X-Ray Anal.* **10**, 9–17.

MEYER, F. (1962). *Z. Phys.* **168**, 29–41.

MIUSKOV, V. F., KONSTANTINOVA, V. P. & GUSEV, A. I. (1969). *Sov. Phys. Crystallogr.* **13**, 791–794.

NEWKIRK, J. B., BONSE, U. & HART, M. (1967). *Advanc. X-Ray Anal.* **10**, 1–8.


*Acta Cryst.* (1973). A**29**, 503

# On the Reliability of the $\sum_2$ Relation. I. Real Structures in $P2_1/c$


BY H. SCHENK

*Laboratory for Crystallography, University of Amsterdam, Nieuwe Prinsengracht* 126, *Amsterdam, The Netherlands*


(*Received* 19 *March* 1973; *accepted* 21 *March* 1973)


It is shown for real structures in $P2_1/c$ that the percentages of failures of the $\sum_2$ relation do not agree with the theoretical values based on the probability formula. Moreover there is some evidence that the probability of a multiple-sign relation is less reliable than that of a single-sign relation. In practice therefore, the probability formula cannot be used to estimate the reliability of a sign indication. An alternative method is proposed, in which only the ten to twenty triplets with highest *EEE* product are used directly. All other signs have to be determined by at least two independent sign indications. It is also shown that in difficult cases the strengthened quartet relation [Schenk (1973). *Acta Cryst.* A**29**, 77–82] is very helpful.


### Introduction

During the last decade the number of successful structure determinations by means of direct phasing has increased enormously. The $\sum_2$ relation

$$\Phi_H = \frac{\sum_K |E_K E_{H-K}|(\Phi_K + \Phi_{H-K})}{\sum_K |E_K E_{H-K}|} \qquad (1)$$

has proved to be the most successful phase relationship. In centrosymmetric space groups a probability formula (6) is associated with the $\sum_2$ relation.

In our laboratory a large number of centrosymmetric structures have been solved by means of the symbolic-addition method (Karle & Karle, 1966), in which a rule of thumb based on the probability formula (6) is used for the acceptance of sign indication. The rule says that a sign indication is accepted if the probability (6) fulfills the condition $P_+(H) > A$ or $P_+(H) < 1 - A$, in which for instance $A = 0{\cdot}97$, as suggested by Karle & Karle (1966). If the probabilities from (6) are reliable then for all structures the same value of $A$ should lead to a correct sign determination. However, in our experience $A$ must be given a wide variety of values